JOURNAL OF MATERIALS SCIENCE 25 (1990) 2321–2334

Correlation between craze formation and mechanical behaviour of amorphous polymers

G. H. MICHLER
Wissenschaftliches Forschungs- und Koordinierungszentrum für Plast- und Elasterzeugung und -anwendung (WKZ) der chemischen Industrie im Kombinat VEB Chemische Werke Buna, 4212 Schkopau, German Democratic Republic
Institut für Festkörperphysik und Elektronenmikroskopie der Akademie der Wissenschaften der DDR, 4050 Halle/S, German Democratic Republic

The formation, growth and fracture of crazes have been studied for several amorphous polymers (PS, PMMA, SAN, NEC, PC). From bulk polymeric materials 0.5 to 5 μm thick sections were prepared and investigated after uniaxial deformation or during *in situ* deformation in a 1000 kV high voltage electron microscope (HVEM). The use of the HVEM also allows one to study irradiation-sensitive polymers (PMMA and PC). The size of crazes (length and thickness), the shape (opening angle at the craze tip, craze thickness profile), the thickness of a pre-craze zone, the structure of the material inside the craze (fibrillar or more homogeneous), and the degree of deformation were measured. Correlations have been found between the type and the size of crazes and their mechanical properties, particularly fracture toughness and elongation at break. There are notable differences between unannealed and annealed samples (SAN and PC) as well as in the craze formation and in the fracture toughness.

1. Introduction

During mechanical loading many amorphous polymers, particularly amorphous brittle or glassy polymers, show the formation of narrow, long bands – the so-called crazes. Unlike cracks, crazes are characterized by an interior structure of strongly plastically deformed polymeric material and by relatively sharp boundaries to the undeformed surroundings.

For studying the structure of crazes optical techniques, in particular electron microscopic methods, have proved very useful. Conventional transmission electron microscopy (TEM) enables the size, shape, and interior structure of crazes to be revealed in detail, requiring, however, very thin specimens of about 0.1 up to 1 μm in thickness [1–3]. Scanning electron microscopy (SEM) detects only large and thick crazes because of the restricted resolving power [4–6].

A very advantageous method is high voltage electron microscopy (HVEM). The high accelerating voltage of 1000 kV makes it possible to investigate relatively thick polymer samples (up to about 10 μm) [7]. Unlike the ultra-thin specimens these semi-thin samples show a mechanical behaviour similar to that of the bulk material. Therefore, HVEM implies advantageous possibilities of revealing micromechanical processes of polymers and of correlating them with ultimate mechanical properties [7, 8].

According to the literature, most electron microscopic studies of crazes were performed using polystyrene (PS) [9, 10] or copolymers of PS [9], e.g. styrene–acrylonitrile copolymers (SAN) [3, 11]. The reason is that PS and its copolymers are far more resistant to electron irradiation than many other polymers. For example, the dosage of high-energetic irradiation (electron or γ-irradiation) for changing any mechanical properties can be 40 times higher for PS than for polyvinylchloride (PVC) and about 500 times higher than for polymethylmethacrylate (PMMA) [12]. Therefore, there are relatively few electron microscopic studies of crazes in PVC, PC, and PMMA. HVEM was used to study the formation, growth, and structure of crazes in PS [7, 10, 13], SAN [7, 14, 15], high-impact polymers [15–17], and recently also in irradiation-sensitive polymers PMMA, PVC, and PC [18].

Recently, formation and break-down of crazes have also been studied by small-angle scattering techniques. Small-angle scattering (of the three different radiations, i.e. of X-rays, neutrons and electrons) has proved to be a useful technique for study crazes, when combined with information only obtainable from TEM [19, 20].

The aim of this paper is to characterize the structure of crazes in different amorphous polymers and to correlate these details with the mechanical behaviour, particularly with the fracture toughness of these polymers.

The fracture toughness of polymers has been widely discussed in the literature. In addition to the type of polymers there are many other factors, determining or influencing the fracture toughness, in particular, the specimen thickness, notch tip radius, molecular weight, temperature, and thermal pretreatment. Correlations between plastic deformation zones near the

0022–2461/90 $03.00 + .12

TABLE I Average mechanical values and Vicat softening temperatures of amorphous polymers

Parameter	PS	PMMA	SAN	NEC	PC
Tensile strength (MPa)	45–55	75–80	60–70	55–65	60–70
Elongation at break (%)	3	2–5	4–5	6–12	50–100
Critical stress intensity factor, K_{Ic} (MPa $m^{1/2}$)	0.7–1.1	0.7–1.6	0.8–1.3	–	2.2
Elastic modulus (MPa)	3500	3500	3600	3000	2000
Impact strength (kJ m^{-2})	18	22	25	20–30	n.f.[1]
Impact strength (notched) (kJ m^{-2})	2	1.8	3	2–3	10–20
Vicat-softening temperature (°C)	100	110	105	130	165

[1] not fractured

notch tip and the mode of failure have been analysed by applying fracture mechanics methods [21]. In addition to these macroscopic correlations, this paper correlates the toughness with deformation zones and processes on a microscopic scale.

2. Experimental technique and samples

From bulk polymeric materials 0.5 to 5 μm thick sections were prepared using an ultramicrotome. The sections were reinforced at their edges with a polyester film and placed in a microtensile device. The specimens were uniaxially deformed, using straining rates between 0.01 and 0.1 sec^{-1}, either outside the HVEM in air under light microscopic control (to prevent any kind of radiation damage), or inside the electron microscope. After or during deformation (i.e. *in situ*) the samples with crazes were investigated in the HVEM with an accelerating voltage of 1000 kV using primary magnifications of up to 80 000. For reducing the electron beam current in the microscope and, therefore, also the radiation damage to the polymeric samples, highly sensitive (double-coated) X-ray films were used. These techniques have been described in more detail elsewhere [7, 10, 22].

The samples investigated are commercial types of several amorphous polymers with molecular weights clearly above the corresponding critical values. Injection-moulded samples were produced from the molten state with a cooling rate of about 10° C min^{-1}. Prior to deformation some of the samples were annealed at temperatures below their glass transition temperatures. Table I contains some characteristic mechanical values and the Vicat temperatures.

SAN as an example of the glassy, brittle polymers and PC of the semi-ductile polymers were tested using fracture mechanics concepts [23]. Instrumented impact tests on three-point bending specimens enabled the fracture toughness properties of these polymers to be determined both without and after annealing. Table II gives the analysed values.

3. Results

3.1. Structure of crazes in different amorphous polymers

In general, crazes are initiated at local points of stress concentration, which can be scratches or notches at the surface, or structural defects, voids or impurities inside the samples. In these places of locally increased stress the amorphous material is transformed into the highly stretched structure of the crazes.

Recently, the structure and the processes of initiation and growth of crazes in PS have been described in detail [10, 13]. Below, only some of the most important features of crazes in PS are quoted because (i) they are usually considered the "prototype" of crazes, and (ii) their structure is compared with those of crazes in the other amorphous polymers.

3.1.1. Polystyrene (PS)

PS is often used mainly because of its good moulding properties and transparency, but it is a very brittle glass at room temperature. The typical interior structure of crazes in PS is shown in Fig. 1 in a 1 μm thick deformed sample (HVEM micrograph): the polymeric material inside the craze is strongly plastically deformed into fibrils. The fibrils are arranged perpendicular to the craze boundaries, are interconnected by thinner fibrils, forming a network, and have diameters mostly between 5 and 10 nm. This regularly fibrillated structure is often considered a typical feature of crazing. Structures may, however, appear that vary essentially: the fibrillar network can be more finely structured or coarsely structured with fibril thicknesses of up to 25 nm and larger voids in between. Many crazes have

TABLE II Fracture toughness values of SAN and PC unannealed and annealed, respectively (fracture mechanics parameters: J integral values J_{Id}, crack opening displacement δ_{Id}; planimetrically measured area below the load–deflection curve a_K) [23]

	SAN		PC	
	unannealed	annealed	unannealed	annealed
J_{Id} (N mm^{-1})	2.2	1.6	7.0	5.0
δ_{Id} (mm)	0.095	0.085	0.195	0.165
a_K (N mm^{-1})	1.5	1.1	4.4	3.3

brighter lines in their middle zone (the "mid rib") and at their boundaries (like the craze in Fig. 1). These variations are described in detail elsewhere [7, 10, 13]. The deformation of the polymeric material inside the crazes was found to lie between 150 and 250% using different methods based on HVEM [10].

The structure first visible ahead of the craze tips, i.e. in the transformation or processing zone of the craze are shown at a higher magnification in Fig. 2a. It shows bright spots like "domains" with diameters between 20 and 50 nm. These "domains" appear brighter than the surrounding material, therefore they are slightly plastically deformed. All domains are arranged in a narrow band, which has almost the same thickness as the diameter of the domains (the band sites at an oblique angle in the specimen and the bright lines on each side of the band are furrows at the upper and lower surfaces of the sample [10]). These zones ahead of the fully developed crazes are called "pre-crazes". They appear as a relatively stable zone and are important for a better understanding of the formation mechanisms of crazes [13, 24].

Values characteristic of the size and structure of crazes in PS are summarized in Table III. The figure below the table defines several sizes used. While some values may vary considerably the domains inside the pre-craze, acting as craze nuclei, and the boundary layer (i.e. the layer between the highly stretched material inside the craze and the non-plastically deformed material in the surroundings) show critical minimum sizes. These critical sizes d_{min} and g_{min} may be considered material constants.

3.1.2. Styrene–acrylonitrile copolymer (SAN)

The samples of SAN under investigation, i.e. copolymers of styrene (S) and acrylonitrile (AN) consisting of 76 wt % S and 24 wt % AN, were produced by mass polymerization. Compared with PS, it shows better mechanical properties with a somewhat higher tensile strength and toughness. Under mechanical load, samples of SAN show deformation zones, partly different from the fibrillated crazes in PS [15]. In front of the crack tips long, broad and wedge-shaped deformation zones appear (see Fig. 3a). Higher magnifications of the interior do not reveal any structure (see Figs 3b and c). Crazes with a fibrillar or network structure very similar to the crazes in PS are shown at the boundary (Figs 3b and c) and outside the

TABLE III Characteristic values of crazes in different amorphous polymers

	PS	PMMA	SAN		NEC	PC	
			unannealed	annealed		unannealed	annealed
Fibrillated crazes (I)							
L_{max} (μm)	500	–	10	100	10	–	10
D_{max} (μm)	10	–	1	1.5	1	–	1
α (deg)	3–6	–	4–12	4–6	4	–	10
$\bar{g}$ (nm)	10–20	–	10–20	10–20	10	–	100
$\bar{l}$ (nm)	10–50	(100)	25–50	40–60	< 50	–	75
d_{min} (nm)	< 20	–	< 50	25	< 50	–	60
Homogeneous crazes (II)							
L_{max} (μm)	–	200	500	–	500	1000	1000
D_{max} (μm)	–	20	60	–	100	> 100	100
α (deg)	–	3–6	15	–	< 15	12	12
$\bar{g}$ (nm)	–	400	300	–	750	1000	1000
dominating type	I	II	I/II	I	I/II	II	II

L_{max} maximum length of crazes.
D_{max} maximum thickness of crazes.
α opening angle at the craze tip.
$\bar{g}$ mean thickness of the boundary layer.
$\bar{l}$ mean distance of the fibrils (fibril long period).
d_{min} minimum diameter of the craze nuclei at the craze tip.

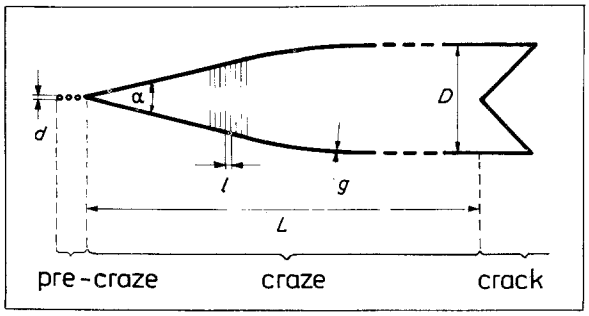

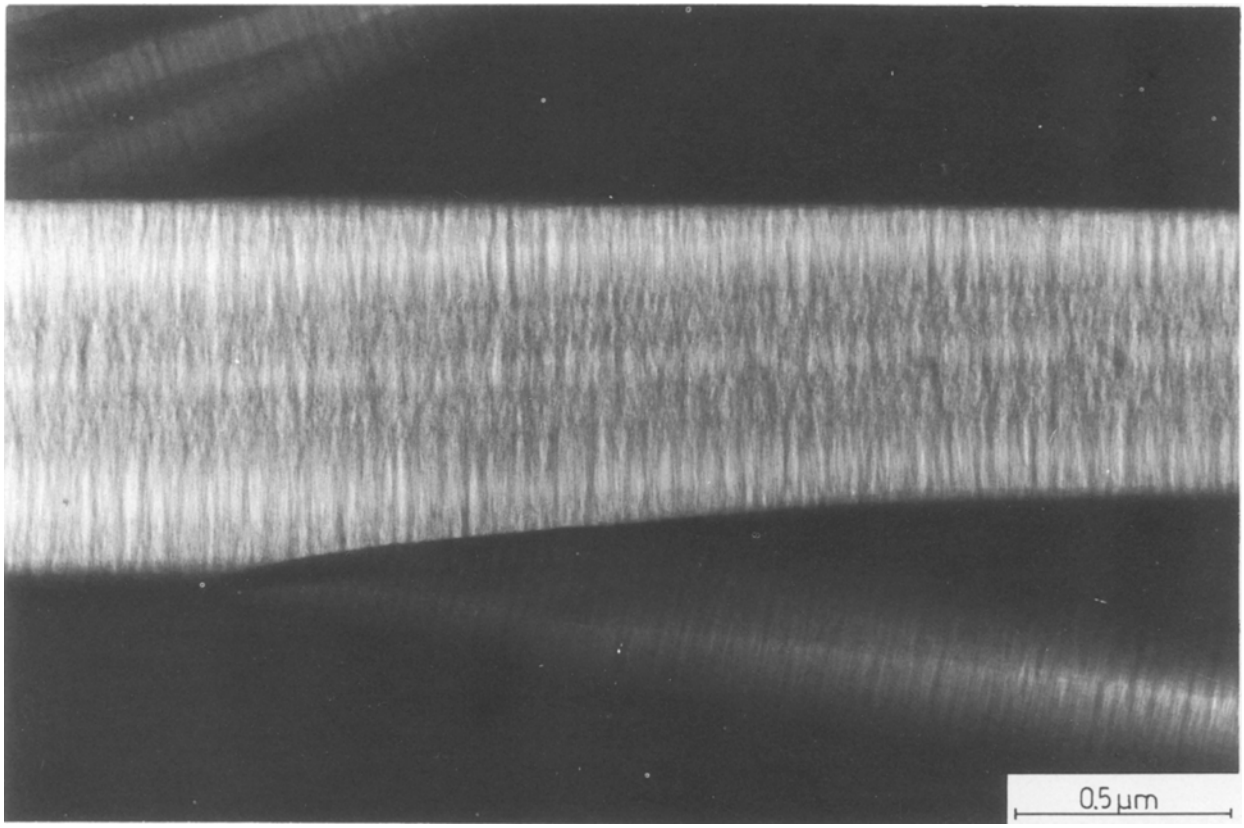

Figure 1 Interior structure of crazes with clearly pronounced fibrillation (1 µm thick section of PS in the HVEM; deformation direction vertical).

"homogeneously" deformed band (Fig. 3b). "Homogeneously" deformed band stands for a deformation band without any visible structure with respect to the actual resolution in the electron microscope (i.e. without structural details coarser than a few nm). Sometimes small crazes exist with a fibrillar structure inside the broad deformation bands (see Fig. 3d). The coexistence of homogeneous zones and fibrillarly stretched crazes is a characteristic of SAN.

The apparently homogeneous or non-structured zones grow attaining considerably larger thicknesses and lengths than the crazes do in PS (see Table III). The deformation of the polymeric material inside the bands was determined by several methods, described in detail elsewhere [10], yielding values of about 100 to 200%. These non-structured bands represent a deformation type, showing the same characteristics as the usual, fibrillated crazes in PS (i.e. they are long, narrow bands vertical to the loading direction, having relatively sharp boundaries to the surrounding material) with the only exception that they lack a pronounced fibrillar structure. In a former study [15] these homogeneous crazes were called crazes II in contrast to the fibrillated crazes which were called crazes I.

Annealing the unloaded SAN samples below their glass-transition temperature T_g (about 378 K) yields a marked change in crazing during subsequent mechanical loading. After annealing for about 100 h at a temperature of 353 K homogeneous crazes no longer appear, only short fibrillated ones. The pattern of some small fibrillated crazes in front of a crack tip in annealed SAN is shown in Fig. 4a, whereas Fig. 4b shows the fibrillar structure of one of these crazes.

The continuous change in type and structure of crazes in annealed samples is demonstrated in Fig. 5. In unannealed SAN large homogeneous crazes preferentially form (see Fig. 5a). After a short annealing time, however, the homogeneous crazes are strongly reduced in size, with smaller fibrillated crazes, however, appearing (see Fig. 5b). After annealing for about 100 h only a few short fibrillated crazes form (see Fig. 5c). The change of the interior structure of the crazes is shown in the highly magnified micrographs Figs 5d and e, respectively: that there is not any structure in the long, broad craze of Fig. 5a is visible with the exception at their tips (Fig. 5d), whereas the small crazes of Fig. 5c show a pronounced fibrillation (Fig. 5e).

The dependence of the type and size of crazes on the annealing time is illustrated in Fig. 6. With increasing annealing time t the maximum length of the homogeneous crazes (L_{II}) decreases to zero, the maximum length of the fibrillated crazes (L_I) increases first and then also decreases. Therefore, the total length of the whole crazed area ($L_I + L_{II}$) in front of a crack tip decreases continuously. Unlike the unannealed material the annealed samples of SAN show a reduced fracture toughness (see Table II).

A high-energetic irradiation of SAN copolymers reduces the fracture toughness. Along with this, the size of crazes is also reduced. The decrease of the length and thickness of homogeneous and fibrillated crazes with increasing ultraviolet irradiation is demonstrated in Table IV. Unlike annealing, UV irradiation does not change the typical deformation character with a coexistence of both types of crazes, but it does decrease the size of the crazes. The

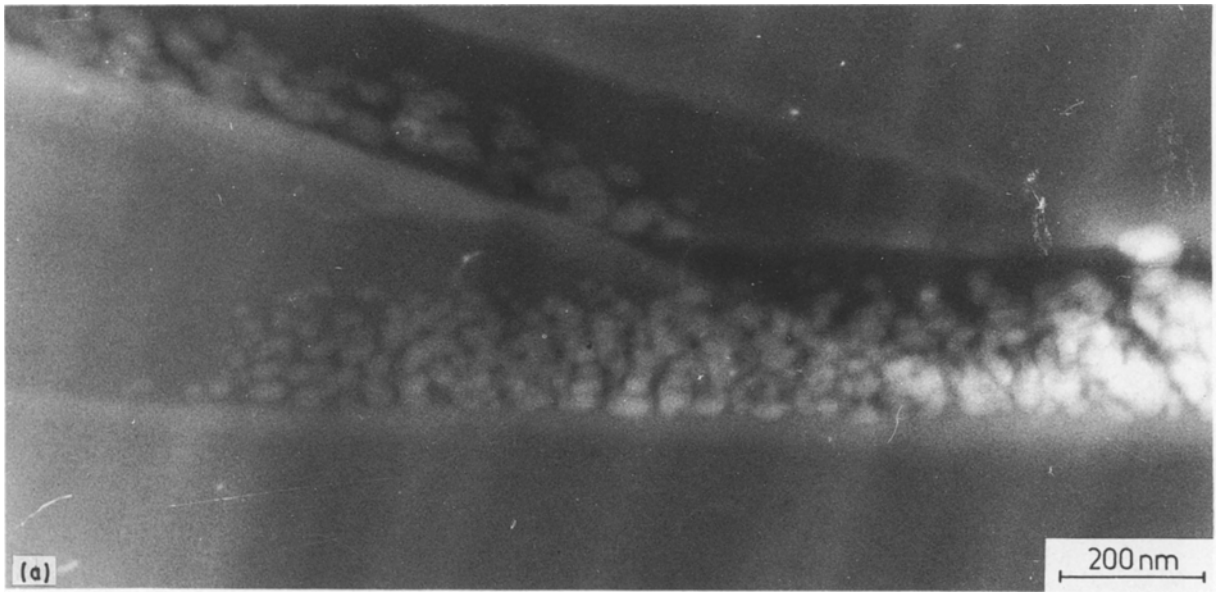

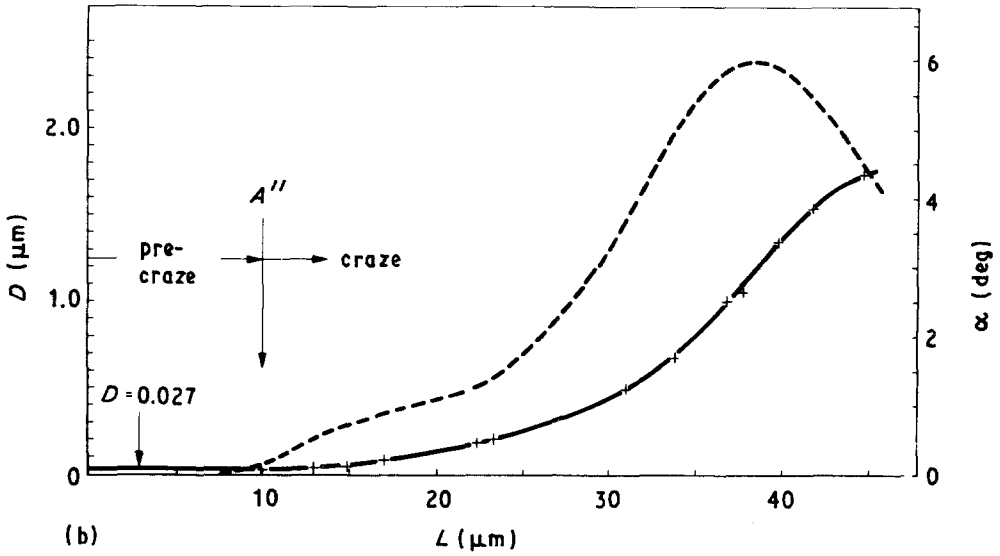

Figure 2 Craze in PS. (a) Higher magnification of the pre-craze ahead of the true craze (the pre-craze is a narrow deformation band inside the sample at an oblique angle to the normal direction of the specimen; deformation direction: vertical). (b) Craze thickness profile (change of the craze thickness, D (——) and the opening angle, α, (– – –) with increasing craze length L; "A" marks the beginning of the true craze).

irradiation of the semi-thin samples inside the HVEM causes a rapid reduction of the craze formation during subsequent deformation and embrittlement.

3.1.3. Norbornene-ethylene copolymer (NEC)

The NEC investigated is an amorphous ethylene copolymer having a statistic composition of N : E = 50 : 50. The mechanical properties classify it as a brittle, glassy polymer (cf. Table I). The high glass-transition temperature T_g is remarkable.

The deformation character of NEC is strikingly similar to that of SAN. There is a predominance of large, apparently homogeneous crazes with a close connection with smaller fibrillated crazes (as in Fig. 3). During the deformation of annealed samples homogeneous crazes no longer form (similar to SAN). The deformation region in front of a crack tip consists solely of lots of small fibrillated crazes (see Fig. 7). Table III gives typical values of these crazes.

3.1.4. Polymethylmethacrylate (PMMA)

PMMA is a transparent glass with good optical properties and is the polymer most intensively studied as far

TABLE IV Decrease of the size of crazes with increasing time of an ultraviolet irradiation of SAN samples

Time of UV irradiation min	Homogeneous crazes			Fibrillated crazes thickness, D (μm)
	Length, L (μm)	Thickness, D (μm)	Opening angle, α (deg)	
0	250	70	20	1.0
30	70	10	10	0.4
60	20	1.5	4	0.3

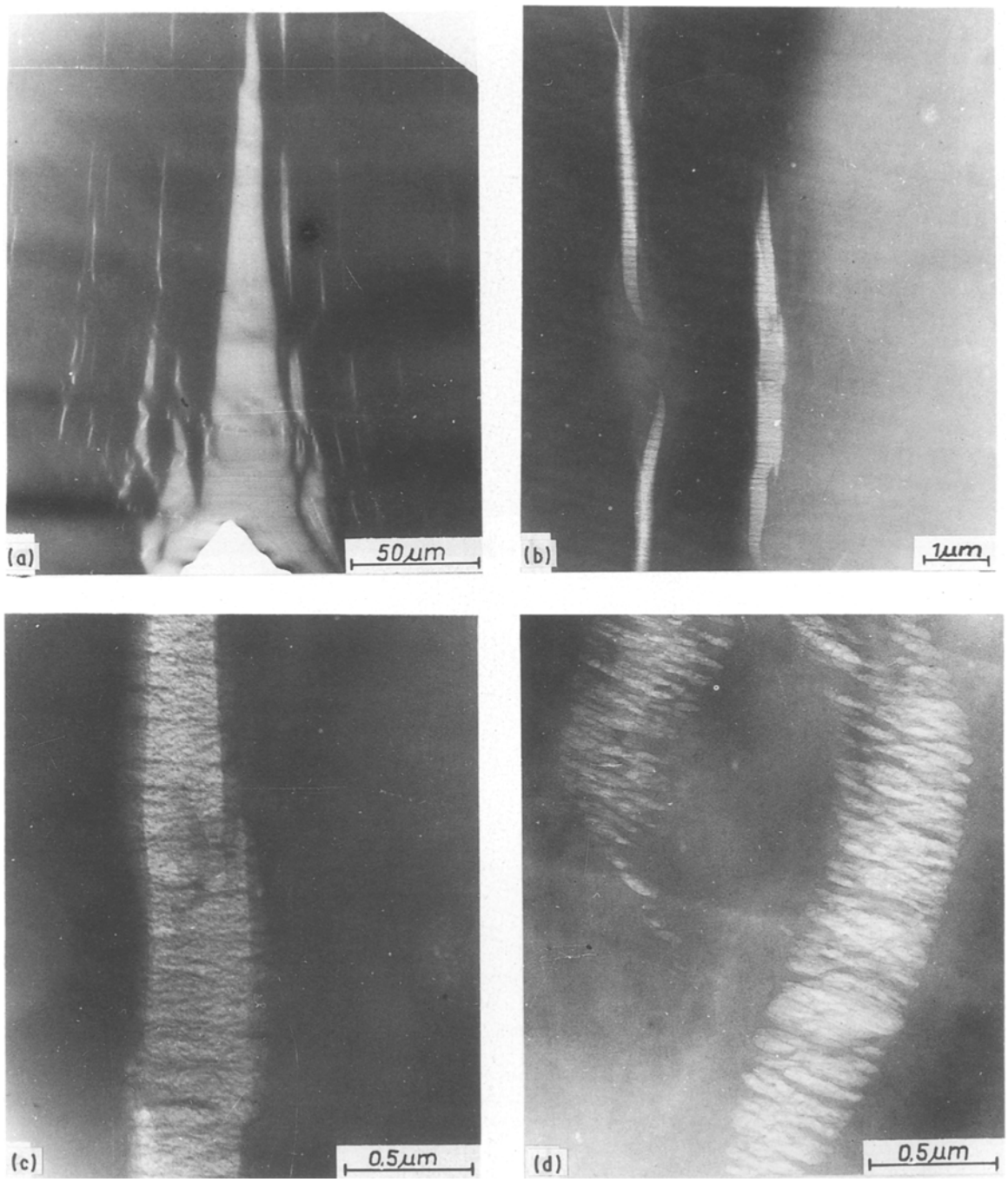

Figure 3 Deformation structures in SAN. (a) Total view of a broad, long and homogeneously stretched deformation zone in front of a crack tip. (b) Crazes of fibrillar structure at the boundary and outside the broad zone. (c) Higher magnification of part of (b). (d) Small crazes with fibrils inside the broad, homogeneously deformed zone (deformation direction is horizontal).

as fracture is concerned, since (i) it is an amorphous glass below 110° C and shows brittle fracture below about 85° C, and (ii) is remarkably consistent in its properties. Under load, in front of a crack samples of PMMA form long, wedge-shaped deformation zones, not showing an interior structure (comparable with Fig. 8a). Only after annealing at 353 K subsequent deformation creates crazes which show a very weak fibrillation (see Fig 8b). The dominant deformation zones, however, are the homogeneous crazes. With increased thickness the crazes of a weakly fibrillated structure change into homogeneous crazes, too.

The high sensitivity of PMMA to electron irradiation causes a rapid formation of microvoids. If the beam current is sufficiently low, the formation of microvoids is first observed inside the deformation bands, whereas higher beam intensities quickly cause many large voids and the damaging of the sample [25, 26].

3.1.5. Polycarbonate (PC)

Like PS and PMMA, PC is an amorphous glass at room temperature, but differs from them in considerable toughness and ductile behaviour under certain circumstances. Plastic yielding of PC is usually connected with the formation of large deformation zones, resembling the homogeneous crazes. Annealed material shows three different types of crazes:

(i) long and broad, homogeneously stretched zones – Fig. 9a;

(ii) small crazes of up to a few μm in length, up to about 1 μm in thickness, and having a coarsely fibril-

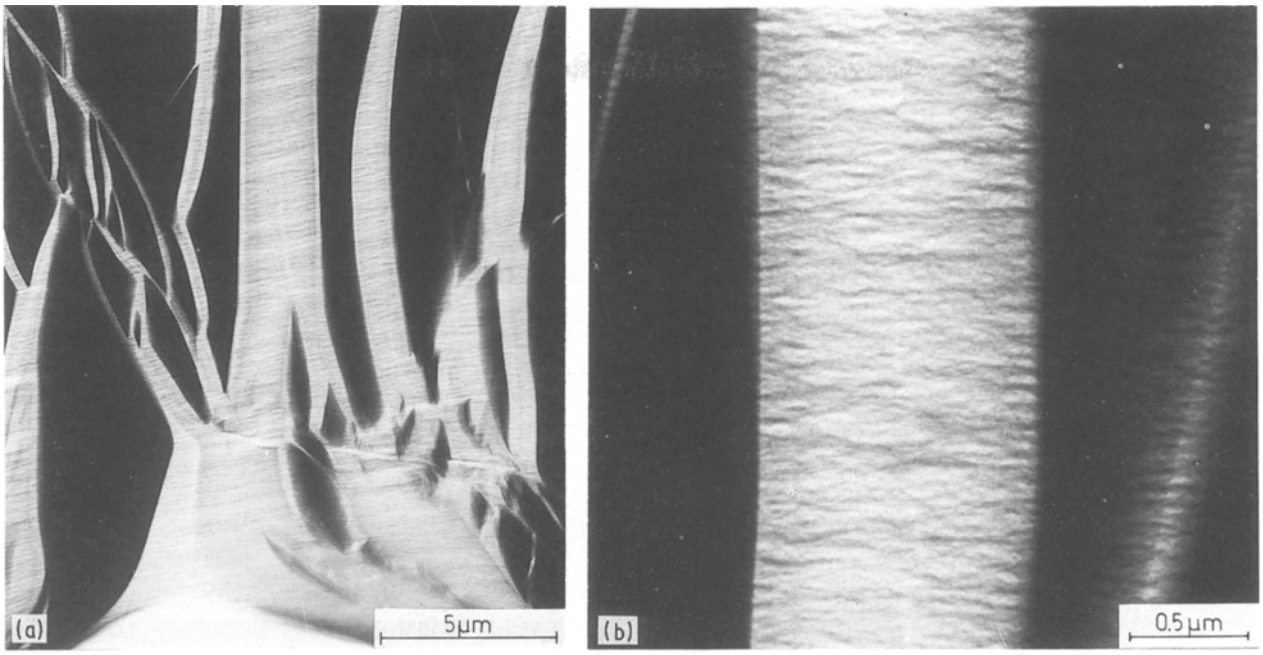

Figure 4 Crazes in SAN after annealing (353 K for 93 h). (a) Lower magnification of crazes in front of a crack tip. (b) Higher magnification of the fibrillar structure of a craze (deformation direction is horizontal).

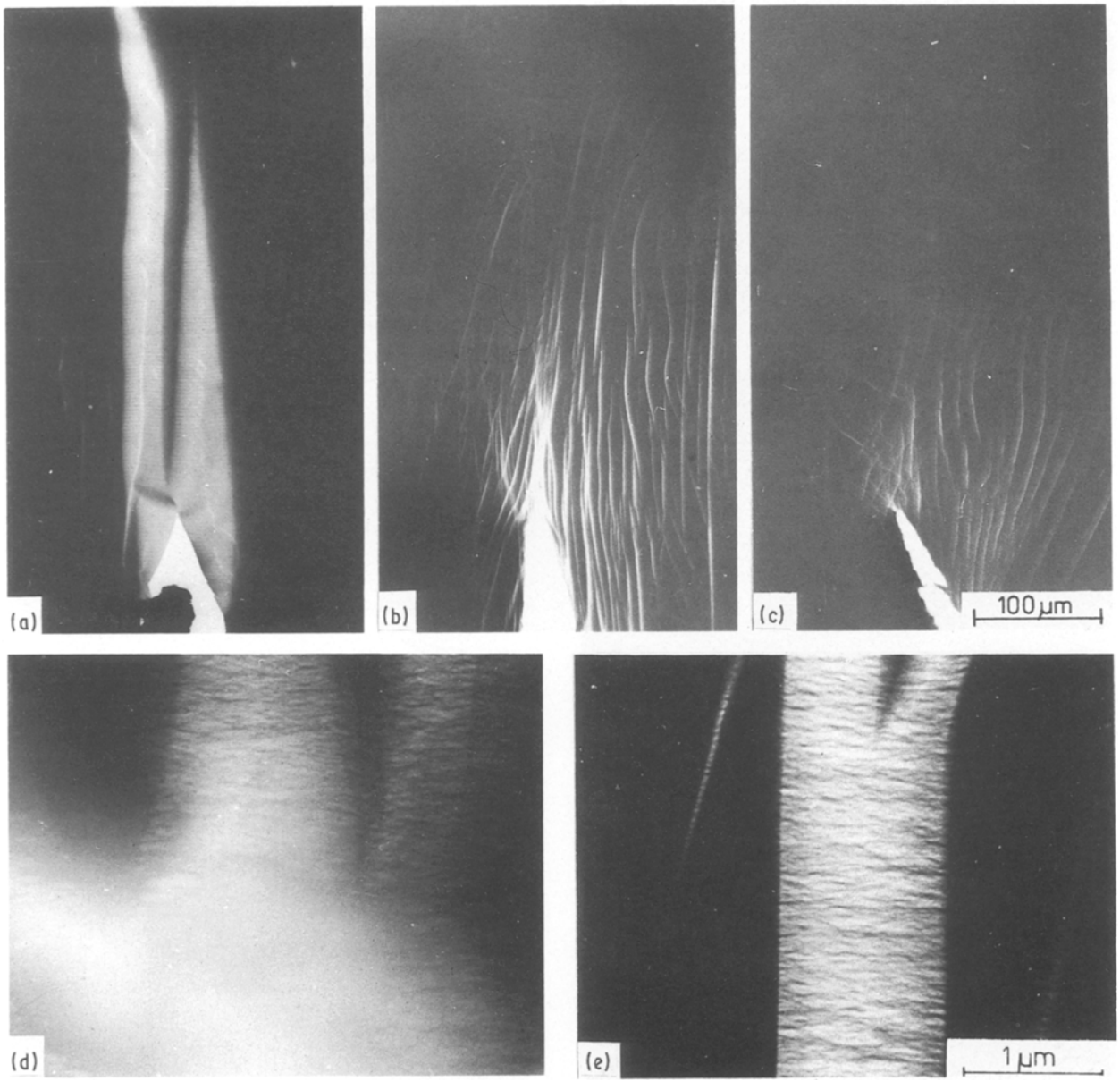

Figure 5 Change of the type and structure of crazes in annealed samples of SAN with increasing annealing time (at 353 K): lower magnification: (a) 0 h, (b) 10 h, (c) 146 h. Higher magnification: (d) 0.5 h, (e) 93 h (deformation direction is horizontal).

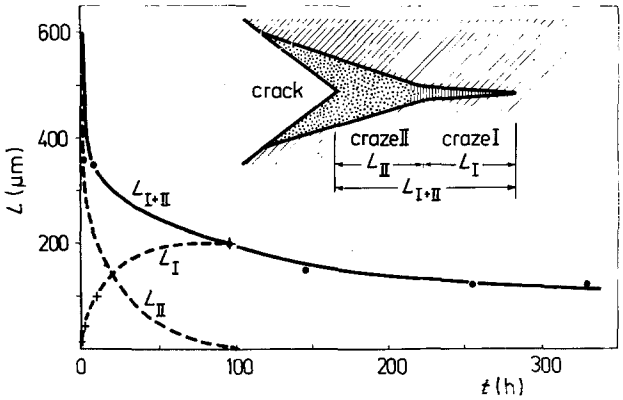

Figure 6 Influence of the annealing time, t, on maximum length of homogeneous crazes (L_{II}), fibrillated crazes (L_I) and the whole crazed zones ($L_I + L_{II}$) in SAN (annealing temperature 353 K).

lated internal structure (inside the larger, homogeneous crazes);

(iii) fibrillated crazes, often appearing at the tip of larger homogeneous crazes – Fig. 9b, and seldom being isolated.

Sizes typical of the crazes are summarized in Table III (omitting the small crazes inside the large, homogeneous crazes, as referred to in (ii)). Values of fracture toughness of unannealed and annealed samples of PC are listed in Table II.

3.2. Initiation and growth of crazes

Initiation of crazes can often be correlated with heterogeneities at the surfaces of the samples (scratches, notches) or in the interior (defects, voids, impurities). Their common characteristic is the ability to produce a local stress concentration under the action of an outer stress. Crazes can, however, also form even if there are no visible defects or heterogeneities. This is possibly due to microstructural defects or local variations of the macromolecular arrangement (e.g. variations of intermolecular connections [27] or of the entanglement density [28]). A locally increased stress is solely important here, high enough to initiate plastic yielding of the polymer and to transform the amorphous material into the plastically stretched structure of crazes. There are different theories and hypotheses about the steps of initiation and formation of crazes, reviewed in for example [9, 13]. In addition to this, electron microscope investigations of craze formation have shown that craze initiation may be considered a nucleation with the starting step of transforming the nuclei into stable domains, at the craze tips visible as bright spots in the electron microscope (cf. Fig. 2a). A theory of craze formation is described based on this in steps of transforming the pre-craze structure into the fibril structure of the developed craze [13] and in connection with results of the glass transition [29, 30].

The growth of crazes proceeds in two stages:

(i) the growth in length (craze tip advance) and

(ii) the growth in thickness.

The growth in length is a propagation of the craze tip perpendicular to the loading direction with a continuous formation of the craze tip structure (as in Fig. 2a) and a subsequent plastic deformation of the polymer material neighbouring the craze nuclei (the pre-craze domains) [13]. The transformation of the pre-craze into fibrils (in the fibrillar crazes) is demonstrated in Fig. 10.

In the literature [3, 31, 32] the mechanism of craze tip advance is often said to be that of the so-called Taylor meniscus instability [33]. This ought not, however, necessarily be assumed; it is pointed out [13] that the above-mentioned repeated nucleation ahead of the craze-tip is most suitable for the formation of the craze structure (unlike formerly discussed complications by Argon [31, 32].

The question of when fibrillar or homogeneous crazes occur is discussed [13, 24, 29] as a function of

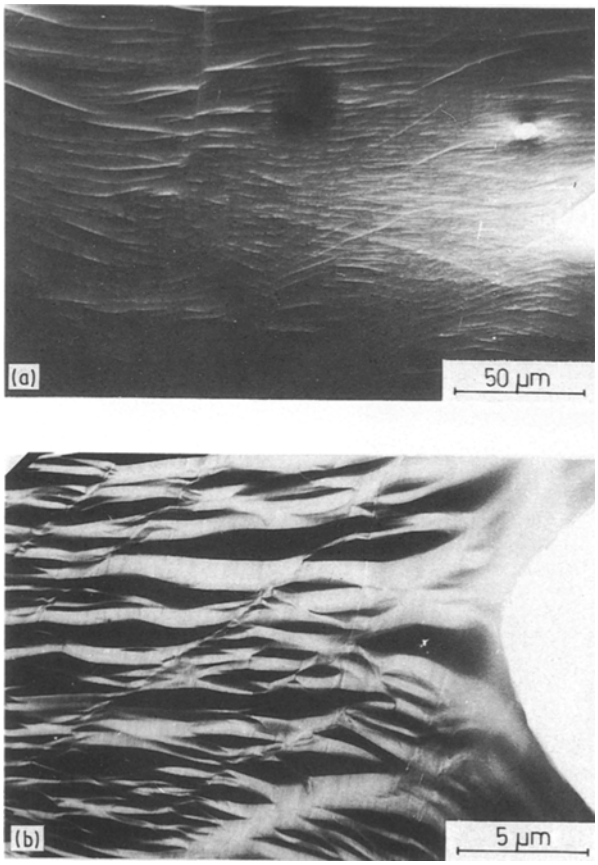

Figure 7 Crazes in a NEC copolymer after annealing (373 K for 9 h) (deformation direction is vertical).

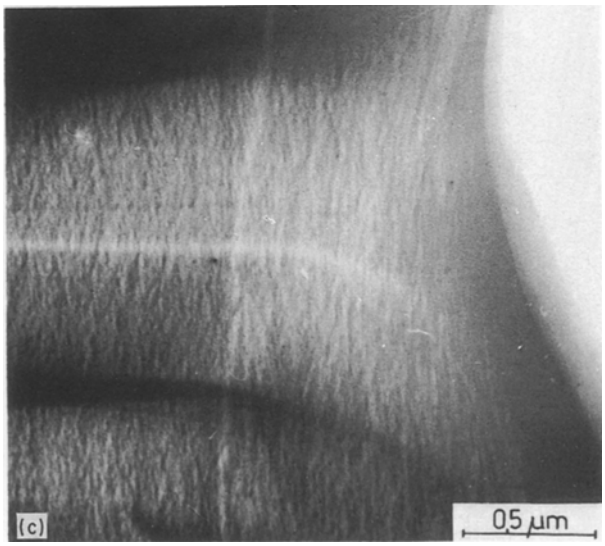

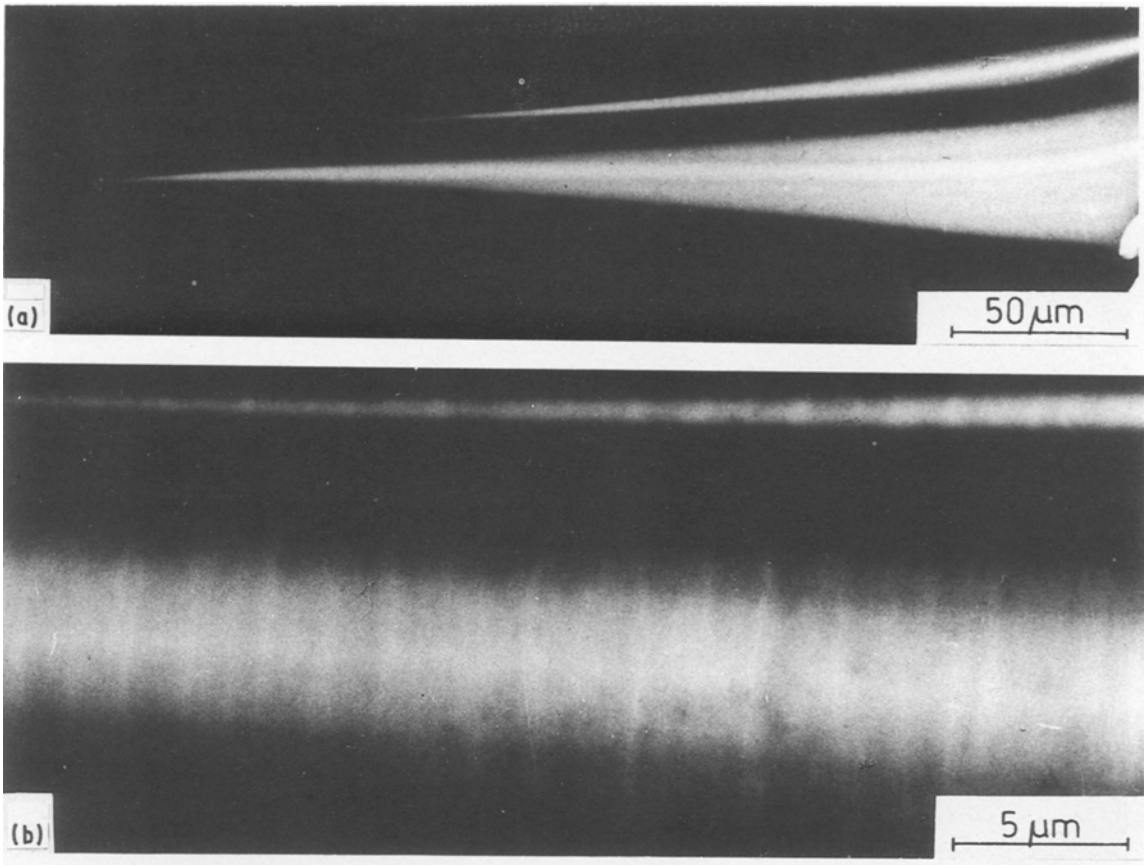

Figure 8 Crazes in PMMA (annealed 353 K for 47 h; deformation direction is vertical); (a) total view of apparently homogeneously stretched crazes, (b) small crazes weakly fibrillated.

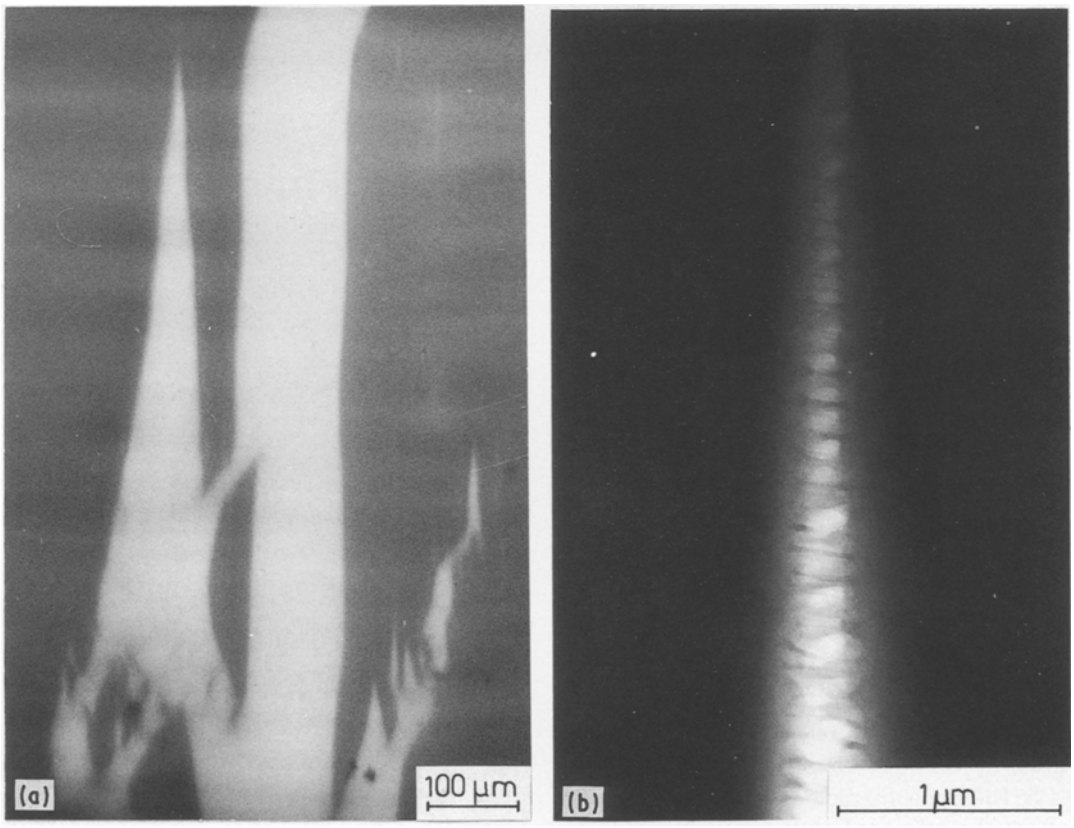

Figure 9 Crazes in PC (annealed at 353 K for 47 h; deformation direction is horizontal) (a) total view of large homogeneously stretched crazes, (b) small fibrillated crazes.

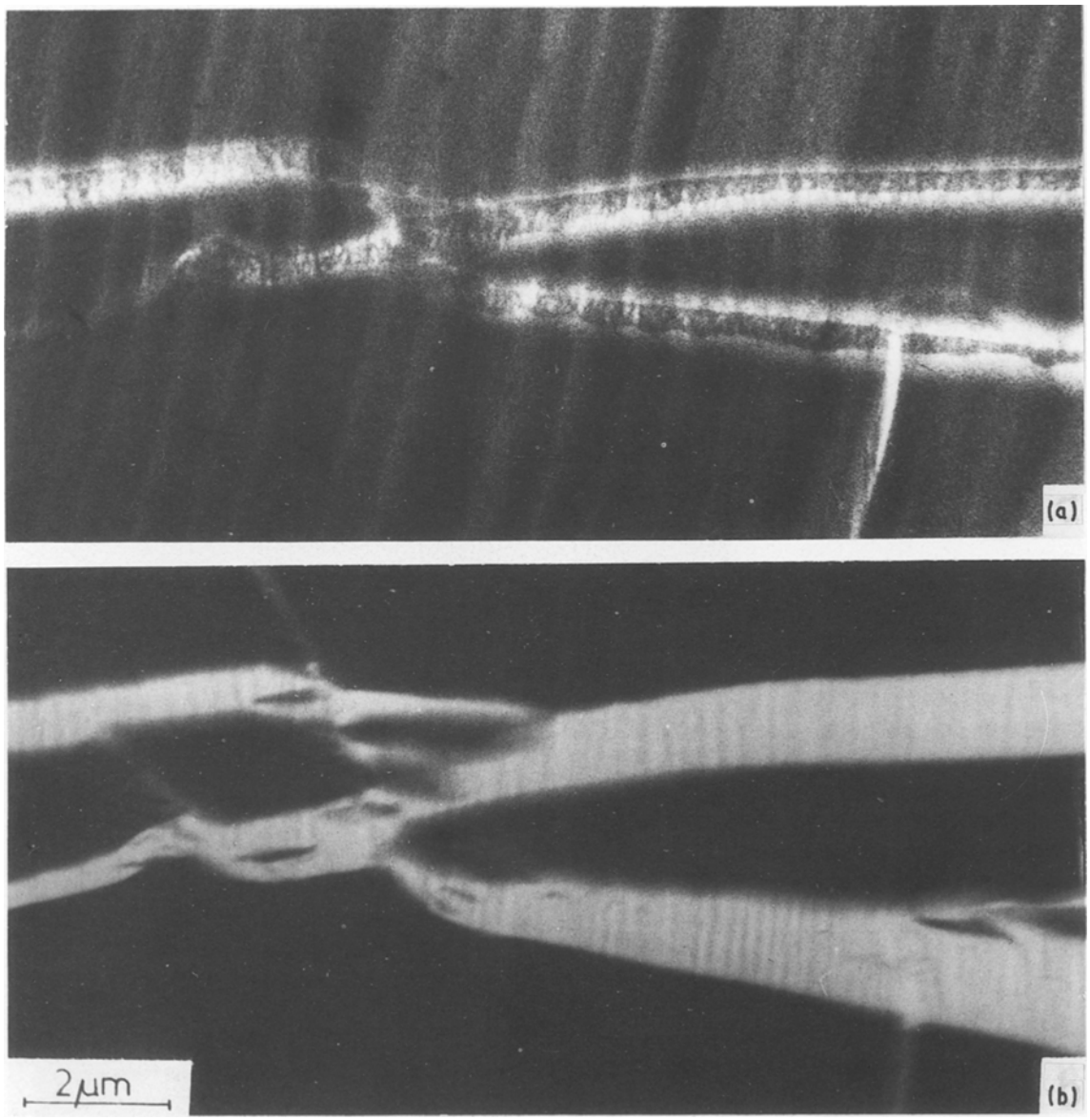

Figure 10 Thickness growth of crazes with the pre craze zones (composed of small domains) changing into the fibrillar structure of the crazes. (*in situ* deformation of a 1 μm thick section of PS; deformation direction is vertical).

the distance of the entanglement points and the stress level locally acting in the sample (cf. Section 4.2.).

Thickness growth occurs by continuously drawing new polymeric material from the craze–bulk polymer interface into the craze associated with a new formation of the structure of the craze material [13, 34]. This continuous surface drawing is usually considered the valid dominant mechanism of craze thickening for dry crazes [3, 35] unlike those crazes which are formed in the presence of solvents, where fibril creep, or another extension of the fibrils [36], is the dominant mechanism. The increase of craze thickness with increasing craze length can be demonstrated by the craze thickness profile. The diagram in Fig. 2b shows the general tendency of PS: first, crazes grow relatively quickly in thickness up to a few μm at opening angles of up to about 6°, and then only slowly. Here it is important to point out that there are characteristic, mean thicknesses of crazes, e.g. about 1 to 2 μm for the fibrillated crazes in PS [10]. Such characteristic thicknesses were also found for the other polymers (cf. Table III). The growth of thickness decreases if the growth is hindered by neighbouring, closely packed crazes.

3.3. Failure of crazes

Failure will occur due to crack initiation and propagation inside the crazes. The starting points of cracks are usually also points of stress concentration, which formerly caused the formation of crazes (e.g. crack tips, surface notches, heterogeneities) or defects inside the crazes. Sometimes fibrils inside the crazes may rupture spontaneously under the influence of a local field of increased stress. Cracks inside the crazes propagate by successive overstressing and rupture of the fibrils, an example of which is shown in Fig. 11. The cracks usually propagate along the central parts of crazes (e.g. along the bright mid-ribs in the fibrillated crazes of PS, where the craze fibrils are extended most), or at the boundaries of the crazes, or in places where the crazes are locally weakened by a higher density of large voids. Cracks inside the crazes propagate quickly almost without absorbing energy. This indicates that the fibrils are relatively saturated in their plastic deformability, having nearly the maximum elongation possible at room temperature.

Ruptured crazes can be identified on fracture surfaces of bulk samples by SEM. Particularly, if the

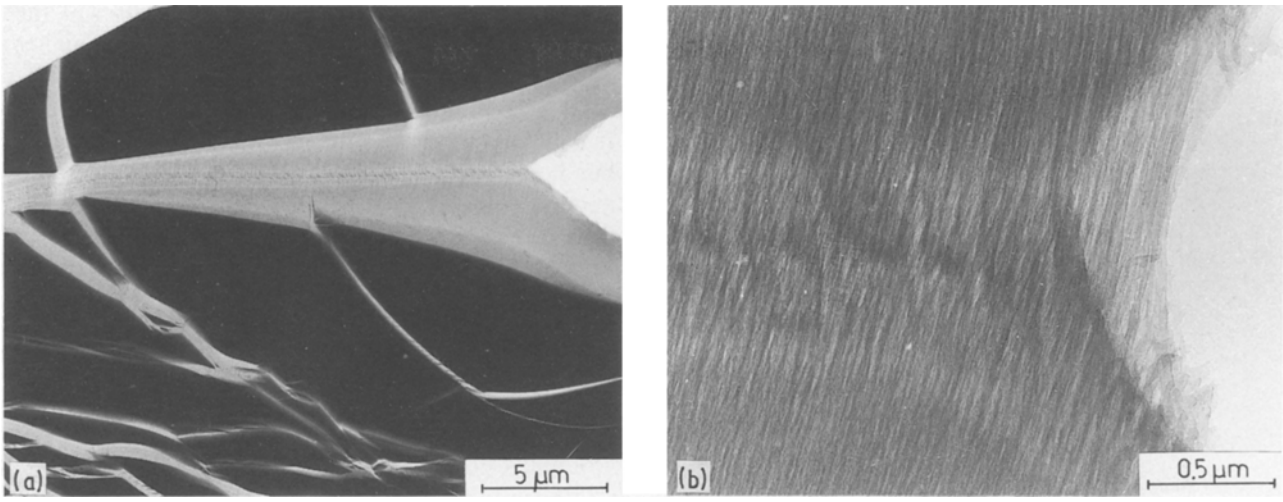

Figure 11 Crack propagation inside a craze in PS. (a) Lower magnification of a craze with a crack tip inside. (b) Higher magnification of the crack tip, revealing successive overstressing and fracture of the fibrils of the craze (deformation direction is vertical).

crack propagates in the middle of the craze, the ruptured and relaxed fibrils of the craze material are visible as small hillocks [37]. The problem of the visibility of crazes on fracture surfaces, in general, has been discussed in many papers, e.g. [38–41].

4. Discussion

4.1. Comparison of crazes in different polymers

According to their microscopic deformation behaviour the amorphous polymers investigated can be divided into three groups:

Group 1: Formation of fibrillated crazes only, both in unannealed and annealed samples. The typical polymer is PS.

Group 2: Formation of "homogeneous" crazes in addition to fibrillated ones in unannealed samples. Annealed samples often show solely fibrillated crazes. Typical examples are SAN and NEC.

Group 3: Formation of long, broad and homogeneous crazes (if there is no macroscopically homogeneous deformation in a necking zone). In annealed samples both types of crazes coexist. Typical polymers are PVC and PC.

Characteristic values of the size and the structure of crazes are listed in Table III. For each polymer about 10 to 20 deformed samples have been analysed. Of all the crazes the fibrillated ones, corresponding to group 1, are those most discussed in the literature (e.g. cf. [9]). A coexistence of the apparently homogeneous and the fibrillated crazes (corresponding to group 2) has been found in SAN by Donald and Kramer [42]. There, the homogeneous crazes are simply called "deformation zones". As, however, they have all the characteristics of crazes, here they are referred to as real crazes [15].

For most of the EM investigations of crazes samples of PS have been used (cf. [9]). The reason is the high resistivity of PS to electron irradiation. Investigations of SAN copolymers are rare. Besides the papers by Kramer *et al.* [3, 42, 43], crazes in SAN have also been described in [11, 44]. In [42, 43] it was pointed out that increasing the strain rate changes the microdeformation of SAN from shear deformation to a competition between shear deformation (or of the formation of narrow "deformation zones") and crazes.

Many years ago, PC has often been studied using surface-active solvents to produce large crazes (solvent crazes), easy to investigate by light microscopy [45–49]. Large surface crazes in PC were also detected by SEM [5, 6]. Using solution-cast films of PC revealed only diffuse shear deformation zones with no crazes present [43, 50].

The case of PMMA is slightly controversial. The present study revealed that PMMA crazes have sizes similar to those of PS crazes (see Table III), but of a more homogeneous (not clearly fibrillated) structure (see Fig. 8). Unlike this, in the literature the crazes in PMMA are usually assumed to have a fibrillar structure, which was only deduced from light microscopic investigations [51–53], but not directly proven by electron microscopy. (Besides, the fibrillar craze shown in [54] is wrongly cited from the original paper and does not originate from PMMA.) On the other hand, the detection of a predominantly homogeneous structure of the crazes correlates with the appearance of crazes in PMMA and rubber-modified PMMA [55, 56], although the sample volume did not obviously increase (an increase of volume or decrease in density, respectively, are macroscopic characteristics of fibrillated crazes).

Inside the large, apparently homogeneously deformed crazes in SAN and PC small crazes with fibrils were detected of smaller lengths and thicknesses, but having larger opening angles α than the isolated crazes with fibrils. They aroused particular interest, because they represent the formation of crazes inside a precrazed, molecularly oriented material. This fact is discussed in more detail in a paper, previously published [26]. However, they are not of primary importance.

The affect of annealing below T_g on the mode of plastic deformation was also examined [43] by light and transmission electron microscopy using thin solution cast films (thickness about 0.4 μm) of SAN, PC, and blends of them. Qualitatively, these thin films

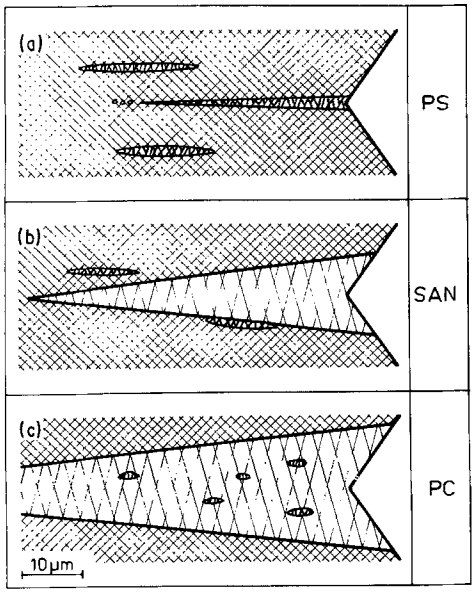

Figure 12 Scheme of different types of crazes in amorphous polymers in front of a crack tip. (a) fibrillar crazes, typical of PS, (b) coexistence of large and apparently homogeneously deformed crazes and small fibrillated crazes, typical of SAN, (c) large, homogeneous crazes with small fibrillated crazes inside, typical of PC (crack tip on the right, assumed deformation direction is vertical).

show a tendency similar to that of the thicker sections from bulk material studied in this paper.

4.2. Correlations between crazing and mechanical behaviour of different polymers

In the order of materials, discussed here (see Table III) the typical deformation zone is observed to change (in unannealed samples): in PS only fibrillar crazes exist; in SAN and NEC crazes with a fibrillar structure coexist with those having a homogeneous structure whereas in PC broad, homogeneous crazes predominate. Besides this, the maximum values of the crazes (maximum length L_{max} and maximum thickness D_{max}), the mean opening angle α, and the minimum thickness, g, of the boundary layer increase. These changes can be correlated with the increase of the fracture toughness of the polymers in this order (PS, SAN and NEC, PC – see Tables I and II). Therefore, the change in the deformation character from fibrillar crazes to more homogeneous ones as well as the increase of the size (or the volume total) of crazes correlate with the increase of the fracture toughness. The homogeneous crazes generally stand for a more ductile behaviour, whereas the fibrillated ones signify more brittleness. The change in the type and size of the crazes with increasing toughness of the polymers investigated is schematically shown in Fig. 12.

A rough macroscopic criterion of the formation of fibrillar or homogeneous crazes, discussed in detail in [24, 25] is the size of the ratio of the yield stress σ_y and the fracture stress σ_f. If $\sigma_y/\sigma_f > 1$, then yielding is preceded by bond rupture and formation of microvoids, and fibrillated crazes appear. In the opposite, if $\sigma_y/\sigma_f < 1$, then local yielding without bond rupture is possible, and homogeneous crazes may appear. The lower yield stress in the second case (in relation to the fracture stress) favours a ductile behaviour and correlates with the above mentioned connection of the formation of homogeneous crazes and the higher toughness of the polymer.

As is mentioned above, PMMA is an exception. It is a glassy, brittle polymer similar to PS or SAN, but it produces crazes of homogeneously stretched material (like PC, but clearly smaller in size). The reason for this exception is not known, but there is possibly a correlation with the high intensity of β-relaxation processes in PMMA relative to PS (discussed in [29, 30]).

The correlation between crazing and toughness, described above, holds true for the comparison of unannealed and annealed samples. Annealing SAN and PC reduces the fracture toughness (see Table II). At the same time the craze character changes from the coexistence of both craze types to only fibrillar ones for annealed SAN and from the dominantly homogeneous crazes to the coexistence of both types in annealed PC (see Table III). In addition, the total size of the crazes is reduced in annealed samples (see Figs 5 and 6).

The plastically deformed material inside the homogeneous crazes suggests the macroscopic effect of cold drawing of polymers taking place in a neck zone. The shoulders of such a microneck make up the craze–bulk polymer interface. In this way, the homogeneous crazes may be considered microscopic presteps of the macroscopic neck zones. In accordance with this is the fact that deformation associated with the formation of necking zones shows a ductile behaviour of the polymers. Another connection of necking zones with crazes is given by the so-called "strain softening", the decrease in stress after starting flow in the neck. After Haward [57], polymers which easily form crazes (like PS and PMMA) show a strong tendency of strain softening (measured under compression). In general, strain softening is a macroscopic sign of the tendency to create crazes.

PC is a typical example of polymers changing the failure mode from ductile to brittle by notching the specimen. Bluntly notched samples (notch tip radius r larger than a critical value r_c) failed in a ductile manner, and sharply notched ones ($r < r_c$) failed in a brittle manner. The value of the critical notch tip radius r_c increases with increasing specimen thickness [58, 59]. Assuming a constant notch tip radius r, sufficiently thin specimens fail in ductile fracture (because $r > r_c$), whereas thick specimens fail in brittle manner (because here $r < r_c$). This ductile–brittle transition can be correlated with the tendency of PC to produce both types of crazes. Under load, thin samples show broad deformation regions or broad, long and homogeneous crazes, responsible for a higher toughness and ductile fracture. With increasing sample thickness the constraint also increases (changing from plane stress conditions into plane strain ones). Therefore, in thick samples the formation of the homogeneous crazes turns out to be more difficult (formation of these homogeneous crazes is a volume-preserving process, demanding contraction in transverse directions), yielding a coexistence of both types of crazes with an increasing tendency of producing fibrillated crazes.

The smaller size of the fibril crazes (cf. Table III) is responsible for the reduced toughness and the transition to the brittle behaviour.

4.3. Role of crazes in enhancing the toughness

Particularly in long, fibrillated crazes cracks propagate very quickly without hindrance (see Fig. 11). In this respect the crazes may be considered the main reason of the brittle behaviour of PS and the other glassy polymers. Pessimists therefore regard crazes as a negative phenomenon. On the other hand, the slight plastic deformation of these polymers is based on the plastic deformation during the formation of crazes. Optimists therefore regard crazes as a positive phenomenon [60], which may cause an increasing fracture toughness (by increasing the number and volume total of crazes).

It was previously shown [16] that there is a strong correlation between the plastic part of energy absorption of glassy and toughened PS and SAN and the total volume of crazes. In the brittle, glassy polymers as e.g. PS, the total energy absorption during deformation is the result of rather the elastic part than of the plastic part (because of the small total amount of crazes). In the more ductile polymers as for example PC the plastic part due to the formation of crazes provides the main contribution to the total energy absorption. Practically realized examples of influencing the total energy absorption, i.e. the fracture toughness, by the amount of crazes are many rubber-modified high-impact polymers (e.g. HIPS and ABS), where the number and the total volume of crazes are strongly increased by incorporating small rubber particles in the brittle polymer matrix. The rubber particles concentrate the stress thus initiating crazes more easily. Not only a qualitative correlation is observed here, but also quantitative correlations were determined between the size and the volume content of the rubber particles, the size, and number (and, therefore, total volume content) of crazes, and toughness, respectively [15–17, 61]. A direct proportionality was also described [21] between the energy of failure in ABS (determined by using the fracture mechanics analysis) and the total volume of crazes (measured directly on the specimen).

5. Conclusions

By investigating amorphous polymeric samples of 0.5 up to 5 μm in thickness, sectioned from bulk material, in a 1000 kV high voltage electron microscope (HVEM) the formation was studied of crazes during mechanical loading of the samples. There is a great variety of structures of crazes in one and the same polymer as well as between different polymers. Nevertheless, characteristic structures and sizes of crazes occurred.

A comparison of the crazes reveals a pronounced correlation between the type of crazes (crazes of (i) fibrillar or (ii) more homogeneous structures within the plastically deformed material) and their size (length and thickness).

In the polymers investigated (PS, PMMA, SAN, NEC, and PC) the formation of crazes provides the main plastic contribution to the fracture toughness. Changing the total amount of crazes therefore influences the fracture toughness of polymers. Negative examples, showing an embrittlement, are annealed samples; positive examples of enhanced toughness are rubber-modified polymers. There is a maximum toughening effect of the amorphous brittle polymers (such as PS, PMMA, SAN), if characteristic sizes of crazes correlate with the diameters of and the distance between the rubber particles. A knowledge of the typical crazing behaviour of polymers enables the toughness to be enhanced. Besides these practical consequences, knowing the structure of crazes particularly at their first stages of formation enables a better interpretation of the processes of initiation and formation of crazes in amorphous polymers and a deeper insight into the molecular processes of deformation.

References

1. P. BEAHAN, M. BEVIS and D. HULL, *Phil. Mag.* **24** (1971) 1267.
2. *Idem, J. Mater. Sci.* **8** (1973) 162.
3. E. J. KRAMER, in "Crazing in Polymers" (*Adv. Polym. Sci.* **52/53**) (Springer-Verlag, Berlin, 1983) p. 1.
4. G. H. MICHLER and K. GRUBER, *Plaste u. Kautschuk* **23** (1976) 346, 496.
5. M. DETTENMAIER and H. H. KAUSCH, *Polymer* **21** (1980) 1232.
6. *Idem, Colloid Polym. Sci.* **259** (1981) 937.
7. G. H. MICHLER, *Kristall u. Technik* **14** (1979) 1357.
8. G. H. MICHLER and V. SCHMIDT, *Plaste u. Kautschuk* **34** (1987) 1.
9. H. H. KAUSCH (Ed.) "Crazing in Polymers" (*Adv. Polym. Sci.* **52/53**) (Springer-Verlag, Berlin, 1983).
10. G. H. MICHLER, *Colloid Polym. Sci.* **263** (1985) 462.
11. P. BEAHAN, A. THOMAS and M. BEVIS, *J. Mater. Sci.* **11** (1976) 1207.
12. E. REXER and L. WUCKEL, "Chemische Veränderung von Stoffen durch energiereiche Bestrahlung", (VEB Deutscher Verlag f. Grundstoffindustrie, Leipzig, 1965).
13. G. H. MICHLER, *Colloid Polym. Sci.* **264** (1986) 522.
14. *Idem, Ultramicroscopy* **15** (1984) 81.
15. *Idem, Acta Polymerica* **36** (1985) 285.
16. *Idem, Plaste u. Kautschuk* **26** (1979) 497, 680.
17. *Idem, Polymer* **27** (1986) 323.
18. *Idem, Plaste u. Kautschuk* **35** (1988) 423.
19. H. R. BROWN, Y. SINDONI, E. J. KRAMER and P. J. MILLS, *Polym. Engng Sci.* **24** (1984) 825.
20. H. R. BROWN, *Mater. Sci. Rep.* **2** (1987) 315.
21. J. G. WILLIAMS, "Fracture Mechanics of Polymers". (Wiley, Chichester, 1984).
22. G. H. MICHLER and Chr. DIETZSCH, *Crystal Res. Technol.* **17** (1982) 1241.
23. G. H. MICHLER and W. GRELLMANN, *Plaste u. Kautschuk* **36** (1989) 120.
24. G. H. MICHLER, *Plaste u. Kautschuk*, **36** (1989) 18.
25. *Idem*, Thesis B, University Halle-Wittenberg (1987).
26. *Idem, Colloid Polym. Sci.* **267** (1989) 377.
27. H. H. KAUSCH, "Polymer Fracture" (Springer-Verlag, Berlin, 1978) (2nd edn 1987).
28. J. F. FELLERS and D. C. HUANG, *J. Appl. Polym. Sci.* **23** (1979) 2315.
29. E. DONTH and G. H. MICHLER, Proceedings IUPAC Symposium MACRO '87, Technical University, Merseburg 1987, IV/Po/75.
30. *Idem, Colloid Polym. Sci.* **267** (1989) 587.
31. A. S. ARGON and M. M. SALAMA, *Phil. Mag.* **36** (1977) 1217.
32. A. S. ARGON, J. G. HANNOOSH and M. M.

SALAMA, Proceedings 4th International Conference Fracture, Waterloo, Canada, 1977. Vol. J, p. 445.
33. G. I. TAYLOR, *Proc. R. Soc. A* **201** (1950) 192.
34. G. H. MICHLER, K. GRUBER, G. POHL and G. KÄSTNER, *Plaste Kautschuk* **20** (1973) 756.
35. B. D. LAUTERWASSER and E. J. KRAMER, *Phil. Mag.* A39 (1979) 469.
36. N. VERHEULPEN-HEYMANS and I. C. BAUWENS, *J. Mater. Sci.* **11** (1976) 7.
37. G. H. MICHLER, in "Strukturabhängiges mechanisches Verhalten von Festkörpern-Glas, Keramik, Polymere" (Akademie, Berlin, 1979) p. 329.
38. D. HULL, *J. Mater. Sci.* **5** (1970) 357.
39. J. MURRAY and D. HULL, *J. Polym. Sci. A* **8** (1970) 583, 1521.
40. R. J. BIRD, G. ROONEY and J. MANN, *Polymer* **12** (1971) 742.
41. M. J. DOYLE, *J. Mater. Sci.* **10** (1975) 300.
42. A. M. DONALD and E. J. KRAMER, *J. Mater. Sci.* **17** (1982) 1871.
43. L. L. BERGER and E. J. KRAMER, *ibid.* **22** (1987) 2739.
44. R. S. MOORE and C. GIENIEWSKI, *J. Appl. Polym. Sci.* **14** (1970) 2889.
45. R. P. KAMBOUR, *Nature (London)* **195** (1962) 1299.
46. *Idem*, *Polymer* **5** (1964) 143.
47. R. P. KAMBOUR and R. R. RUSSELL, *Polymer* **12** (1971) 237.
48. E. L. THOMAS and S. J. ISRAEL, *J. Mater. Sci.* **10** (1975) 1603.
49. N. VERHEULPEN-HEYMANS and I. C. BAUWENS, *ibid.* **11** (1976) 1.
50. A. M. DONALD and E. J. KRAMER, *ibid.* **16** (1981) 2967.
51. W. DÖLL, "Crazing in Polymers", edited by H. H. Kausch (*Adv. Polym. Sci.* **52/53**) (Springer, Berlin, 1983) p. 105.
52. H. OYSAED and I. E. RUYTER, *J. Mater. Sci.* **22** (1987) 3373.
53. R. SCHIRRER, *ibid.* **22** (1987) 2289.
54. E. PASSAGLIA, *J. Phys. Chem. Solids* **48** (1987) 1075.
55. B. E. READ and G. D. DEAN, *Polymer* **25** (1984) 1679.
56. C. B. BUCKNALL, I. K. PARTRIDGE and M. V. WARD, *J. Mater. Sci.* **19** (1984) 2064.
57. R. N. HAWARD (ed), "Physics of Glassy Polymers" (Applied Science, London, 1973).
58. H. HYAKUTAKE and H. NISITANI, *Jpn SOC. Mech. Eng. Int. J.* **30** (1987) 29.
59. H. R. BROWN, *J. Mater. Sci.* **17** (1982) 469.
60. R. P. KAMBOUR, *J. Polym. Sci., Macromol. Rev.* **7** (1973) 1.
61. G. H. MICHLER, *Acta Polymerica* **36** (1985) 325.

Received 8 February
and accepted 24 August 1989